Desalination and Water Treatment
www.deswater.com

doi: 10.5004/dwt.2018.22798

126 (2018) 157–163
September

PVA/SiO_2-coated stainless steel mesh with superhydrophilic–underwater superoleophobic for efficient oil–water separation

Xinying Zhang, Chaoqun Wang, Xiaoyan Liu*,†, Jinhua Wang*,†, Chenying Zhang, Yuling Wen

College of Environmental and Chemical Engineering, Shanghai University, 99 Shangda Road, Shanghai 200444, China, emails: lxy999@shu.edu.cn (X. Liu), jinhuawang@staff.shu.edu.cn (J. Wang), zxyshu@shu.edu.cn (X. Zhang), 124123400@qq.com (C. Wang), 275343476@qq.com (C. Zhang), 276947095@qq.com (Y. Wen)

Received 9 November 2017; Accepted 12 July 2018

ABSTRACT

Polyvinyl alcohol (PVA)/SiO_2-modified stainless steel mesh was fabricated to use as an underwater superoleophobic membrane for a high effective separation of oily wastewater. The fabricated membranes showed superhydrophilic properties in air and underwater superoleophobicity. The underwater oil contact angles of modified membranes were up to 156.6°. The maximum separation efficiency of PVA/SiO_2-modified stainless steel mesh for hexane, cyclohexane, diesel, soybean oil, lubricating oil, and silicone oil was 99.4%, 99.3%, 99.6%, 99.0%, 98.6%, and 98.0%, respectively. In addition, the PVA/SiO_2-coated stainless steel mesh still retained high separation efficiency (above 95%) for hexane after 100 separation cycles. This membrane also exhibited durable underwater superoleophobicity in the pH range from 4 to 10. The membranes were prepared in a single step by the dip-coating method. The PVA/SiO_2-coated meshes had high efficiency, high flux, and good reusability. The modified membranes could effectively separate oil from water without depending on any extra power. This membrane could be a promising product for the cleanup of oil spills and oily wastewater.

Keywords: Underwater superoleophobic; PVA; SiO_2; Stainless steel mesh

1. Introduction

A large amount of oily wastewater are being released everyday due to the industrial material processing [1], as well as frequent crude oil leakage [2], such as daily chemical, metallurgical, petrochemical, and food industries. On one hand, the oily wastewater generated from industrial material processing has become one of the most significant ways in waste of water resources [3]. On the other hand, the frequent oil spill accidents have a long term and lethal influence on people and even the whole ecosystem [4]. Therefore, it is very imperative to handle oily wastewater appropriately. Oil–water separation is an effective approach for the reuse of oil and water. Conventional methods, such as electric field, gravity separation, and centrifugation, have been widely used as separation technologies. However, these approaches have a lot of limitations due to the generation of secondary pollutants, low separation efficiency, and large size [5,6]. Meanwhile, the membrane separation technology, due to its promising advantage for oil–water separation, is rapidly developing.

Superhydrophobic and superoleophilic membranes, based on their low energy cost and high oil removal efficiency, could be used to effectively separate oil from contaminated oil–water mixtures by filtering [7,8]. Nevertheless, these superhydrophobic membranes for oil–water separation were inevitably fouled by oils on account of their high oils affinity, thereby resulting in the decrease of the separation efficiency [9,10]. Recently, Xue et al. [11] inspired by fish scales to design

* Corresponding author.
† Equal contributors.

a "water-removing" filtration mesh with superhydrophilic and underwater superoleophobic properties, which can solve the problem of membrane fouling. Based on this innovative method, hydrogels [11,12], polymer membranes [13–16], hydrophilic nanoparticles [17,18], and metal oxides [19–21] had been used to prepare the underwater superoleophobic materials. These materials can be used for oil–water mixtures, and most of them have high separation efficiency. Nevertheless, hydrogels and polymer membranes are susceptible to mechanical damage, and they also have low flux. Some researchers used meshes as substrates and then coated them with polymers and nanoparticles to enhance their mechanical strength and flux. Hou et al. [22] used poly(diallyldimethylammonium chloride)/halloysite nanotubes-modified mesh to fabricate a new synthetic underwater superoleophobic material with high durability and chemical stability. Liu et al. [23] prepared a chitosan/SiO_2-coated mesh which showed a stability in harsh corrosive water. These works inspired us to prepare a polymer–nanoparticles composite material with high flux, stability, and durability.

Polyvinyl alcohol (PVA) is a kind of green and environmentally friendly hydrophilic polymer materials. Due to its hydrophilicity, PVA membranes have been fabricated to be used in many fields, such as biomedicine [24], antifouling [25], pervaporation [26], etc. Fan et al. [27] fabricated an underwater superoleophobic oil–water separation membrane with PVA and cellulose filter paper by a simple crosslinking process. The membrane was effective for oil–water separation in complex environment. The low mechanical strength and flux of filter paper were not benefit for filtration. Gu et al. [28] used PVA/SiO_2 nanocomposite coating to fabricate a durable underwater superoleophobic surface. This coated glass material showed a higher underwater superoleophobicity and exhibited an underwater self-cleaning performance. However, it was not reported that PVA/SiO_2 nanocomposite was appropriate for the porous materials to separate oily wastewater.

In this work, a simple modification method was provided to fabricate a stable and durable oil–water separation membrane. Stainless steel mesh was used as substrate to prepare the underwater superoleophobic oil–water separation membrane. The stainless steel mesh substrates can increase the separation efficiency and durability for oil–water separation. PVA/SiO_2 nanocomposite coatings were used to provide stainless steel mesh a rougher surface and hydrophilic chemical constitution. The filtration flux, separation efficiency, chemical property, and reusability of modified stainless steel mesh were characterized in this work. It would demonstrate extensive application prospect for different kinds of oil–water mixture wastewater.

2. Materials and methods

2.1. Materials

Stainless steel meshes (bore diameter 50 μm) were obtained from Shanghai Hongxiang Metal Mesh Co., Ltd (Shanghai, China). The reagents including SiO_2 (Aerosil R200, hydrophily, particle size < 20 nm) and PVA (molecular weight of 84,000–89,000, 88% hydrolyzed) were purchased from Shanghai Sinopec Co., Ltd (Shanghai, China). Glutaraldehyde (biochemical reagent, 25% in water), 1, 2-dichloroethane (analytical reagent [AR]), acetone (AR), absolute ethyl alcohol (AR), hexane (AR), cyclohexane (AR), hydrochloric acid (AR), and water black pigment (AR) were purchased Shanghai Sinopharm Chemical Reagent Co (Shanghai, China). The deionized water was self-made in the laboratory. Diesel (density at 20°C = 0.8170 g cm^{-3}, viscosity = 6.51 $mm^2 s^{-1}$), soybean oil (density at 20°C = 0.9255 g cm^{-3}, viscosity = 7.26 $mm^2 s^{-1}$), lubricating oil (density at 20°C = 0.7881 g cm^{-3}, viscosity = 47–57 $mm^2 s^{-1}$), and silicone oil (density at 20°C = 0.9630 g cm^{-3}, viscosity = 92–108 $mm^2 s^{-1}$) was obtained from Minghe petrol station of Sinopec in Baoshan district (Shanghai, China).

2.2. Methods

2.2.1. Preparation of PVA coating

The PVA powder (1 g) was dissolved in 100 mL of deionized water with magnetic stirring at room temperature. A total of 1 wt% of PVA aqueous solution was obtained after the complete dissolution of PVA.

2.2.2. Preparation of PVA/SiO_2 coating

SiO_2 (5 g) was dispersed in 100 mL of absolute ethyl alcohol with magnetic stirring for 30 min. The SiO_2–alcohol suspension was charged into 1 wt% of PVA aqueous solution with stirring, and then the mixture was ultrasonically dispersed by using an ultrasonic cleaner for 10 min. The pH of the obtained solution was adjusted to 3 by hydrochloric acid. Then the glutaraldehyde (0.5 mL) was added into the mixture with vigorous stirring.

2.2.3. Preparation of PVA/SiO_2 meshes

The stainless steel meshes were cut into square shape (6 cm × 6 cm). Then they were cleaned with acetone, absolute ethyl alcohol, and deionized water for 30 min, respectively, by using an ultrasonic cleaner. After that, they were dried at 60°C for 30 min to remove the moisture completely. The stainless steel meshes were dipped into the PVA/SiO_2 coating solution for 15 s and dried at 60°C for 2 h.

2.3. Characterizations

2.3.1. Attenuated total reflection-Fourier transformed infrared spectroscopy (ATIR-FTIR) spectra

The surface functional groups of the sample were detected using Nicolet-380 spectrometer (Thermo Fisher Ltd, USA) at room temperature. The spectra were performed in the range from 4,000 to 400 cm^{-1} with an accumulation of 40 scans at 16 cm^{-1} resolution. The membranes were set on the sample stage, and the overall test process was performed by OMNIC software.

2.3.2. Scanning electron microscopy

The surface morphology of the samples coated with Au was investigated using scanning electron microscopy (SEM, SU-1510, Hitachi Ltd, Japan). Before measurements,

the machine was vacuumized by turbo molecular pump. The samples were cut into square shape (1 cm × 1 cm) and adhered on the conducting resin. Then, the obtained samples were sprayed by sputter coater for 5 min. SEM images were examined at an accelerating voltage of 20 kV.

2.3.3. Energy dispersive X-ray spectrometer

Energy dispersive X-ray spectrometer (EDS) analysis of the samples was carried out on the same machine with SEM (SEM, SU-1510, Hitachi Ltd, Japan) to determine the chemical composition of the samples. The measurements were obtained in width and depth of 15 mm and the take-off angle of 35°.

2.3.4. Contact angle

The contact angles (CA) and oil contact angles (OCA) of the surface carried out using CA measuring device (OCA30, Dataphysics, Germany). The measurements of water CA in air were carried out with an 8 μL droplet of deionized water. For the underwater OCA, oil (1, 2-dichloroethane) droplets (8 μL) were syringed out to the surfaces of the samples which were immersed in a silica glass cuvette filled with water. The final results were obtained with the average of three different monitoring points.

2.3.5. The stability experiment

The stability experiment was characterized by the OCA of the samples. Before measurements, the modified meshes were immersed in acidic, alkaline, and neutral environment for 12 h, 24 h, and 48 h, respectively. The pH of acidic, alkaline, and neutral environment was 4, 7, and 10, respectively.

2.3.6. Oil–water separation experiment

The oil–water separation was proceeded by using the improved sand-core filter. The prepared stainless steel meshes were fixed between two glass tubes. The oil–water mixture (about 100 mL of oil and 100 mL of water were mixed through a shake process) was poured into the upper glass beaker. The reusability measurements were obtained by repeating the above steps. After every experiment of the oil–water separation, the prepared mesh was washed by deionized water for later test. The mesh flux was tested in the process of separation efficiency experiment. The separation efficiency of the samples was calculated after each cycle. The whole process was proceeded in the gravity conditions. The oil–water separation efficiency of six oils, such as hexane, cyclohexane, diesel, soybean oil, lubricating oil, and silicone oil, were examined in this work.

3. Results and discussion

3.1. Functional groups

The ATR-FTIR spectra of stainless steel meshes, PVA-modified meshes, and PVA/SiO_2-modified meshes are shown in Fig. 1. The stainless steel meshes did not have any obvious characteristic peak. The new absorption peaks at 3,369, 2,925, 1,190, 1,069, 805, and 464 cm^{-1} were observed in

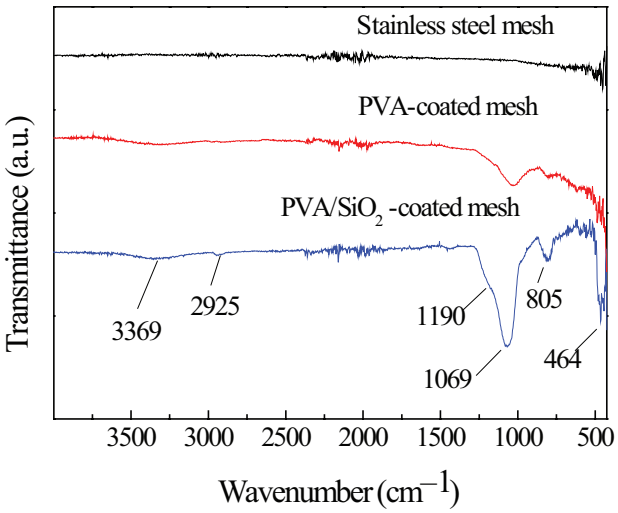

Fig. 1. ATR-FTIR spectra of stainless steel mesh, PVA-coated stainless steel mesh, and PVA/SiO_2-coated stainless steel mesh.

PVA/SiO_2-modified meshes. The absorption bands at 3,369 and 2,925 cm^{-1} corresponded to the stretching vibration of hydroxyl groups (–OH groups) [29,30], which were the residual hydroxyl groups of PVA chains after crosslinking between PVA and glutaraldehyde. They were observed both in PVA and PVA/SiO_2-modified meshes. The peak at 1,069 cm^{-1} was the characteristic peak of the C–O groups [31]. Compared with the absorption peaks in the spectrum of PVA-modified meshes, obvious enhancement of absorption peaks could be observed from PVA/SiO_2-modified meshes at 1,069 cm^{-1}. This was due to that the stretching vibration of Si–O–Si groups [32] was overlapped with C–O groups at 1,069 cm^{-1}. New absorption peak appeared at 805 and 464 cm^{-1}, which were the stretching vibration of the Si-O [32,33]. The absorption at 1,190 cm^{-1} indicated the stretching vibration of –C–O–C– groups. These results implied the crosslinking reaction between PVA and glutaraldehyde [28,29].

3.2. Morphology and chemical constitution

The SEM images of the samples are displayed in Figs. 2(a) and (b). It was observed that stainless steel meshes had a smooth surface (Fig. 2(a)), and the modified stainless steel meshes wrapped up by the coating (Fig. 2(b)). This result showed that PVA/SiO_2 nanocomposite successfully coated on the surface of mesh. A great deal of micro-folded structure was formed by SiO_2 nanoparticle, which made the surface of the modified meshes rougher. In addition, the PVA/SiO_2 nanocomposite was uniformly coated onto the surface of the modified meshes.

The EDS analysis is displayed in Figs. 2(c) and (d). The elements C, O, Fe, Cr, and Si were observed in spectrogram (Figs. 2(c) and (d)). The elements C, Fe, and Cr were the compositions of the stainless steel. After coating, the weight percentage of C increased to 28.36%, and the new element O was observed in the meshes. This was due to that the PVA is successfully coated on the surface of the meshes. The increased weight percentage of element Si in the PVA/SiO_2-coated meshes was from SiO_2 nanoparticle.

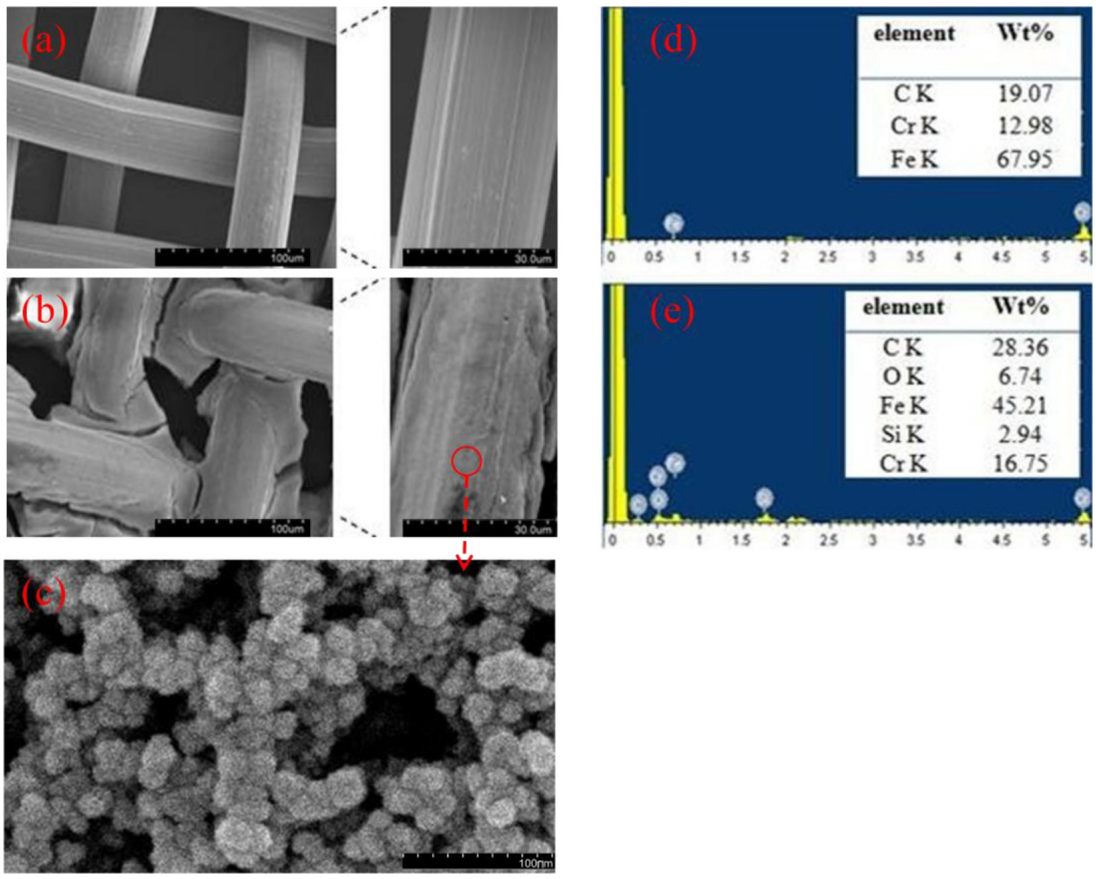

Fig. 2. Morphology and chemical constitution of PVA/SiO_2-coated stainless steel mesh (a) ×500 and ×1,000 SEM micrographs of stainless steel mesh, (b) ×500 and ×1,000 SEM micrographs of PVA/SiO_2-coated stainless steel mesh, (c) ×100,000 SEM micrographs of PVA/SiO_2-coated stainless steel mesh, (d) EDS micrographs of stainless steel mesh, and (e) EDS micrographs of PVA/SiO_2-coated stainless steel mesh.

3.3. Wettability and stability

The wetting properties of the samples are shown in Fig. 3. The results of CAs are displayed in Figs. 3(a)–(c). The stainless steel mesh showed hydrophobicity in the air with the CA of 100.9°, and the CA of the PVA-coated mesh was 31.6°. It showed that PVA coating has a high hydrophilic, but it could not improve the mesh to achieve superhydrophilic property. However, Fan et al. [27] fabricated a superhydrophilic filter paper using PVA as modifier. It was due to that the filter paper was a hydrophilic material with itself. After modified by PVA/SiO_2 nanocomposite coating, the CA of the PVA/SiO_2-coated stainless steel mesh decreased to 0°. It exhibited a superhydrophilic property. It implied that the addition of SiO_2 nanoparticle could improve the hydrophilicity of the PVA coating.

The underwater OCAs of the samples are shown in Figs. 3(d)–(f). The underwater OCAs were examined by dropping 1, 2-dichloroethane onto the surface. The underwater OCAs of PVA-coated meshes and PVA/SiO_2-coated meshes were 132.9°, 139.1°, and 156.6°, respectively. The results implied that the PVA and PVA/SiO_2 coating could both improve the underwater oleophobic property. Meanwhile, it was worth noting that the PVA/SiO_2-coated meshes exhibited underwater superoleophobicity. The SiO_2 nanoparticle could improve the hydrophilicity of PVA [28], which in turn could also constitute some micro or nanostructure [28,34]. The formed bump structure and folded structure supplied higher surface roughness.

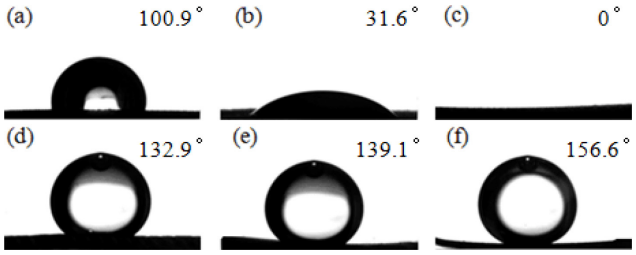

Fig. 3. Contact angle (CA) and underwater oil contact angle (OCA) measurements of the samples. (a) CA of stainless steel mesh in the air, (b) CA of PVA-coated stainless steel mesh in the air, (c) CA of PVA/SiO_2-coated stainless steel mesh in the air, (d) underwater OCA of stainless steel mesh, (e) underwater OCA of PVA-coated stainless steel mesh, and (f) underwater OCA of PVA/SiO_2-coated stainless steel mesh.

The stability of the membranes is an important property for separation. The stability of the PVA/SiO_2-coated meshes was investigated in different solutions with pH 4,

7, and 10. The underwater OCAs of the PVA/SiO_2-coated meshes after immersing are shown in Fig. 4. The underwater OCAs of stainless steel meshes decreased to 152.8°, 151.5°, and 151.2° in pH 4, 7, and 10, respectively, after 48 h. Though the underwater OCA decreased slightly, all of the immersed PVA/SiO_2-coated meshes still exhibited underwater superoleophobicity. This result implied that this PVA/SiO_2-coated meshes could continuously work in acidic, alkaline, and neutral environment for a relative long time (48 h), and this PVA/SiO_2 nanocomposite could be stably coated onto the surface of stainless steel meshes.

3.4. Separation efficiency and reusability

To further demonstrate the separation efficiency of the modified meshes, a series of studies was investigated. The separation process of oil–water with the PVA/SiO_2-coated meshes is shown in Fig. 5. As presented in Fig. 5(a), the PVA/SiO_2-coated meshes were fixed between two glass beakers. Then, the 200 mL of oil–water mixture (about 100 mL of oil with the yellow color and 100 mL of water dyed black using Nigrosine water soluble) was poured onto the upper glass beaker (Fig. 5(b)). Water permeated through the modified meshes quickly, and oil was repelled and stayed on the mesh (Fig. 5(c)). It is shown that the PVA/SiO_2-coated meshes had a good separation efficiency.

The separation efficiencies of the PVA/SiO_2-coated meshes for hexane, cyclohexane, diesel, soybean oil, lubricating oil, and silicone oil are shown in Fig. 6. The separation efficiency was expressed by the ratio of the separated amount

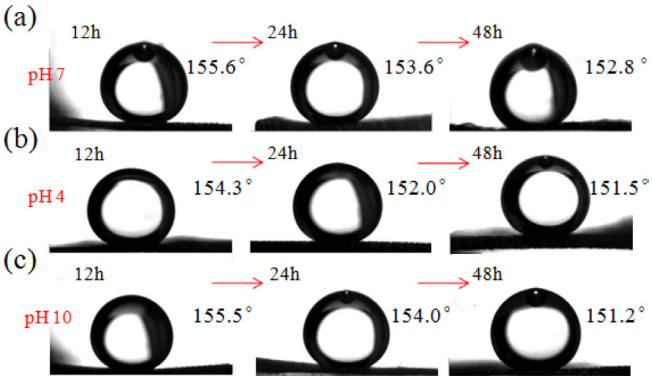

Fig. 4. The stabilities of PVA/SiO_2-coated stainless steel mesh in different pH. (a) Underwater OCA of PVA/SiO_2-coated mesh in pH 7, (b) underwater OCA of PVA-coated mesh in pH 4, and (c) underwater OCA of PVA/SiO_2-coated mesh in pH 10.

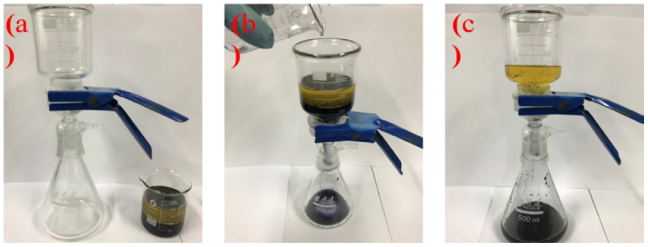

Fig. 5. The separation process of PVA/SiO_2-coated mesh for oil–water separation.

and the initial amount of oil. The flux was gotten by recording the passing time of the 100 mL water in 200 mL of oil–water solution. The maximum separation efficiencies of the PVA/SiO_2-coated meshes for hexane, cyclohexane, diesel, soybean oil, lubricating oil, and silicone oil could reach 99.4%, 99.3%, 99.6%, 99.0%, 98.6%, and 98.0%, respectively. The separation efficiency declined with the viscosity of oils increasing. The PVA-modified filter paper had a high separation efficiency, which can reach 99.9% [27]. However, the maximum flux was only 63 L m^{-2} h^{-1} [27]. The flux of the PVA/SiO_2-coated meshes could reach 9,523 L m^{-2} h^{-1}. Compared with many polymeric membranes, the PVA/SiO_2-coated meshes display a relatively high fluxes in oil–water separation [34–36].

The reusability of the PVA/SiO_2-modified stainless steel mesh was shown in Fig. 7. After 50 cycles, the separation efficiency of the modified meshes for hexane could still remain above 98%. And after 100 cycles, the separation efficiency of

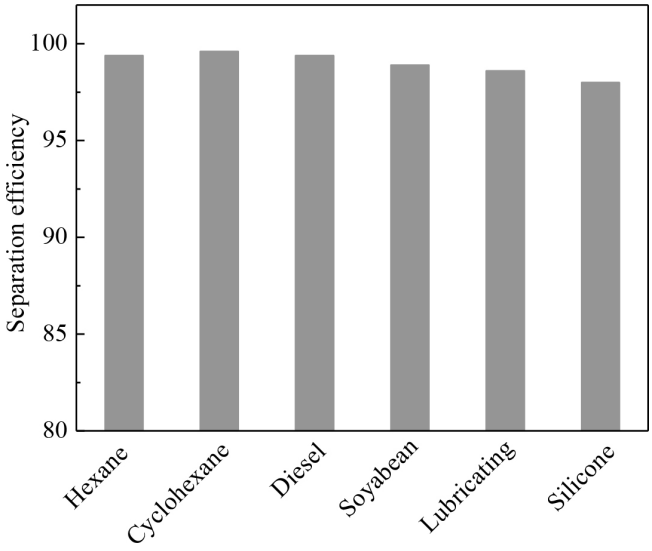

Fig. 6. The separation efficiency of PVA/SiO_2-coated mesh for different oils.

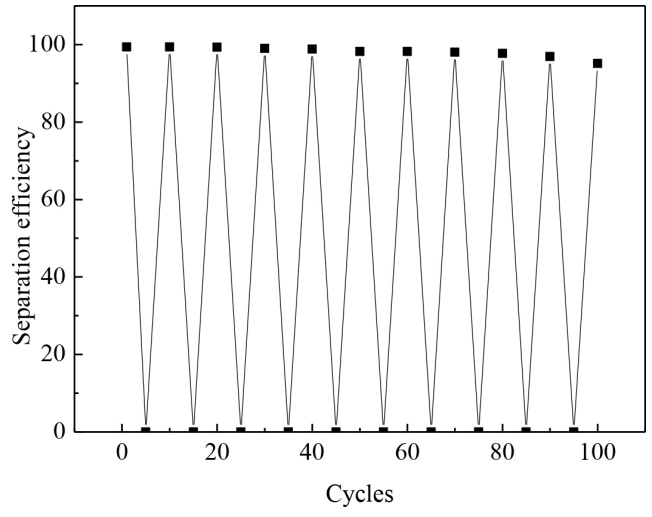

Fig. 7. The reusability of PVA/SiO_2-coated mesh.

the modified meshes declined to 95.7%. In general, the PVA/SiO_2-coated meshes showed a high reusability compared with some polymeric or metal membranes. Wu et al. [30] used crosslinked PVA coating to fabricate a PVA-modified fabric. The separation efficiency of the modified fabric could reach above 99%. However, after 10 cycles, the separation efficiency declined below 98%. And the SiO_2–polyurethane (PU)-coated mesh [37] and TiO_2–PU-coated mesh [38] could reach 98.0% and 97.5% after 40 cycles, which was a little lower than the PVA/SiO_2-coated meshes. Hence, the filtration flux, separation efficiency, stability, and reusability of the PVA/SiO_2-modified stainless steel mesh showed a huge advantage, which would be potential for oil–water separation.

4. Conclusions

This work provided a novel and simple method for fabricating the superhydrophilic–underwater superoleophobic PVA/SiO_2 nanocomposite coatings on stainless steel mesh for oil–water separation. Compared with previously reported methods, this method was much easier to carry out. The CAs of the PVA/SiO_2-modified stainless steel meshes changed from hydrophobicity (CA = 100.9°) to superhydrophilicity (CA = 0°). Meanwhile, the underwater OCAs of the modified membranes could reach 156.6°, which increased 33.7°. The maximum separation efficiency of the modified membranes could reach 99.4%, 99.3%, 99.6%, 99.0%, 98.6%, and 98.0%, for hexane, cyclohexane, diesel, soybean oil, lubricating oil, and silicone oil, respectively. The PVA/SiO_2-coated meshes had high efficiency for oil–water separation, which were appropriate for different oils. In addition, the modified membranes have a high flux and reusability. After 100 cycles, the separation efficiency could still reach above 95%. Consequently, it is believed that this underwater superoleophobic PVA/SiO_2 nanocomposite-coated stainless steel meshes could be a promising product for the cleanup of oil spills and oily wastewater based on their easy assembling and outstanding properties.

Acknowledgment

This work was funded by the National Natural Science Foundation of China (Nos. 21677093 and 41373097) and Natural Science Foundation of Shanghai (No. 18ZR1414100).

References

[1] Y.Z. Zhu, D. Wang, L. Jiang, J. Jin, Recent progress in developing advanced membranes for emulsified oil/water separation, NPG Asia Mater., 6 (2014) e101.
[2] A.A. Al-Majed, A.R. Adebayo, M.E. Hossain, A sustainable approach to controlling oil spills, J. Environ. Manage., 113 (2012) 213–227.
[3] V. Singh, M.K. Purkait, C. Das, Cross-flow microfiltration of industrial oily wastewater: experimental and theoretical consideration, Sep. Sci. Technol., 46 (2011) 1213–1223.
[4] I.B. Ivshina, M.S. Kuyukina, A.V. Krivoruchko, A.A. Elkin, S.O. Makarov, C.J. Cunningham, T.A. Peshkur, R.M. Atlas, J.C. Philp, Oil spill problems and sustainable response strategies through new technologies, Environ. Sci. Processes Impacts, 17 (2015) 1201–1219.
[5] Z.X. Xue, Y.Z. Cao, N. Liu, L. Feng, L. Jiang, Special wettable materials for oil/water separation, J. Mater. Chem. A, 2 (2014) 2445–2460.
[6] M. Padaki, R.S. Murali, M.S. Abdullah, N. Misdan, A. Moslehyani, M.A. Kassim, N. Hilal, A.F. Ismail, Membrane technology enhancement in oil–water separation. A review, Desalination, 357 (2015) 197–207.
[7] C. Yeom, Y. Kim, Purification of oily seawater/wastewater using superhydrophobic nano-silica coated mesh and sponge, J. Ind. Eng. Chem., 40 (2016) 47–53.
[8] D.K. Li, Z.G. Guo, Stable and self-healing superhydrophobic MnO2@fabrics: applications in self-cleaning, oil/water separation and wear resistance, J. Colloid Interface Sci., 503 (2017) 124–130.
[9] Q.L. Ma, H.F. Cheng, A.G. Fane, R. Wang, H. Zhang, Recent development of advanced materials with special wettability for selective oil/water separation, Small, 12 (2016) 2186–2202.
[10] B.Y. Chen, G.N. Ju, E. Sakai, J.H. Qiu, Underwater low adhesive hydrogel-coated functionally integrated device by a one-step solution-immersion method for oil–water separation, RSC Adv., 5 (2015) 87055–87060.
[11] Z.X. Xue, S.T. Wang, L. Lin, L. Chen, M.J. Liu, L. Feng, L. Jiang, A Novel superhydrophilic and underwater superoleophobic hydrogel-coated mesh for oil/water separation, Adv. Mater., 23 (2011) 4270–4273.
[12] C. Teng, X.Y. Lu, G.Y. Ren, Y. Zhu, M.X. Wan, L. Jiang, Underwater self-cleaning PEDOT-PSS hydrogel mesh for effective separation of corrosive and hot oil/water mixtures, Adv. Mater. Interfaces, 1 (2014) 1400099.
[13] Y.B. Peng, F. Guo, Q.Y. Wen, F.C. Yang, Z.G. Guo, A novel polyacrylonitrile membrane with a high flux for emulsified oil/water separation, Sep. Purif. Technol., 184 (2017) 72–78.
[14] T. Yuan, J.Q. Meng, T.Y. Hao, Z.H. Wang, Y.F. Zhang, A scalable method toward superhydrophilic and underwater superoleophobic PVDF membranes for effective oil/water emulsion separation, ACS Appl. Mater. Interfaces, 7 (2015) 14896–14904.
[15] W.B. Zhang, Y.Z. Zhu, X. Liu, D. Wang, J.Y. Li, L. Jiang, J. Jin, Salt-induced fabrication of superhydrophilic and underwater superoleophobic PAA-g-PVDF membranes for effective separation of oil-in-water emulsions, Angew. Chem. Int. Ed., 53 (2014) 856–860.
[16] J.Q. Hao, C.F. Xiao, J. Zhao, L. Chen, Fabrication and properties of graphene-coated polypropylene hollow fiber membranes, Desal. Wat. Treat., 68 (2017) 353–360.
[17] U.B. Gunatilake, J. Bandara, Efficient removal of oil from oil contaminated water by superhydrophilic and underwater superoleophobic nano/micro structured TiO_2 nanofibers coated mesh, Chemosphere, 171 (2017) 134–141.
[18] Q.L. Ma, H.F. Cheng, Y.F. Yu, Y. Huang, Q.P. Lu, S.K. Han, J.Z. Chen, R. Wang, A.G. Fane, H. Zhang, Preparation of superhydrophilic and underwater superoleophobic nanofiber-based meshes from waste glass for multifunctional oil/water separation, Small, 13 (2017) 1700391.
[19] D.L. Tian, X.F. Zhang, Y. Tian, Y. Wu, X. Wang, J. Zhai, L. Jiang, Photo-induced water-oil separation based on switchable superhydrophobicity-superhydrophilicity and underwater superoleophobicity of the aligned ZnO nanorod array-coated mesh films, J. Mater. Chem., 22 (2012) 19652–19657.
[20] F. Zhang, W.B. Zhang, Z. Shi, D. Wang, J. Jin, L. Jiang, Nanowire-haired inorganic membranes with superhydrophilicity and underwater ultralow adhesive superoleophobicity for high-efficiency oil/water separation, Adv. Mater., 25 (2013) 4192–4198.
[21] X. Xiong, J.G. Bao, S.H. Omer, G. Hui, Z. Yu, W. Hong, Study for adsorption behaviors of emulsion oil on a novel ZrO2/PVDF modified membrane, Desal. Wat. Treat., 57 (2016) 11736–11745.
[22] K. Hou, Y.C. Zeng, C.L. Zhou, J.H. Chen, X.F. Wen, S.P. Xu, J. Cheng, Y.G. Lin, P.H. Pi, Durable underwater superoleophobic PDDA/halloysite nanotubes decorated stainless steel mesh for efficient oil–water separation, Appl. Surf. Sci., 416 (2017) 344–352.
[23] J. Liu, P. Li, L. Chen, Y. Feng, W.X. He, X.H. Yan, X.M. Lu, Superhydrophilic and underwater superoleophobic modified chitosan-coated mesh for oil/water separation, Surf. Coat. Technol., 307 (2016) 171–176.

[24] D.Z. Yang, Y.N. Li, J. Nie, Preparation of gelatin/PVA nanofibers and their potential application in controlled release of drugs, Carbohydr. Polym., 69 (2007) 538–543.
[25] A.W. Qin, X. Li, X.Z. Zhao, D.P. Liu, C.J. He, Engineering a highly hydrophilic PVDF membrane via binding TiO_2 nanoparticles and a PVA layer onto a membrane surface, ACS Appl. Mater. Interfaces, 7 (2015) 8427–8436.
[26] T.F. Ceia, A.G. Silva, C.S. Ribeiroa, J.V. Pinto, M.H. Casimiro, A.M. Ramos, J. Vital, PVA composite catalytic membranes for hyacinth flavour synthesis in a pervaporation membrane reactor, Catal. Today, 236 (2014) 98–107.
[27] J.B. Fan, Y.Y. Song, S.T. Wang, J.X. Meng, G. Yang, X.L. Guo, L. Feng, L. Jiang, Directly coating hydrogel on filter paper for effective oil–water separation in highly acidic, alkaline, and salty environment, Adv. Funct. Mater., 25 (2015) 5368–5375.
[28] Y.J. Gu, J.H. Yang, S.X. Zhou, A facile immersion-curing approach to surface-tailored poly(vinyl alcohol)/silica underwater superoleophobic coatings with improved transparency and robustness, J. Mater. Chem. A, 5 (2017) 10866–10875.
[29] Q. Wang, Y.J. Fu, X.X. Yan, Y.J. Chang, L.L. Ren, J. Zhou, Preparation and characterization of underwater superoleophobic chitosan/poly(vinyl alcohol) coatings for self-cleaning and oil/water separation, Appl. Surf. Sci., 412 (2017) 10–18.
[30] J.D. Wu, W. Wei, S.F. Zhao, M.Y. Sun, J.P. Wang, Fabrication of highly underwater oleophobic textiles through poly(vinyl alcohol) crosslinking for oil/water separation: the effect of surface wettability and textile type, J. Mater. Sci., 52 (2017) 1194–1202.
[31] M. Shateri-Khalilabad, M.E. Yazdanshenas, Fabricating electroconductive cotton textiles using graphene, Carbohydr. Polym., 96 (2013) 190–195.
[32] H.K. Tchakoute, C.H. Ruscher, Mechanical and microstructural properties of metakaolin-based geopolymer cements from sodium waterglass and phosphoric acid solution as hardeners: a comparative study, Appl. Clay Sci., 140 (2017) 81–87.
[33] M.T. Taghizadeh, M. Vatanparast, Nafion/sulfonic acid functionalized SnO_2/SiO_2 nanocomposite for mitigation of membrane chemical degradation in PEM fuel cells, J. Mater. Sci. - Mater. Electron, 28 (2017) 778–786.
[34] B.B. Li, X.Y. Liu, X.Y. Zhang, W.B. Chai, Stainless steel mesh coated with silica for oil–water separation, Eur. Polym. J., 73 (2015) 374–379.
[35] Y.Z. Zhu, W. Xie, J.Y. Li, T.L. Xing, J. Jin, pH-Induced non-fouling membrane for effective separation of oil-in-water emulsion, J. Membr. Sci., 477 (2015) 131–138.
[36] T. Yuan, J.Q. Meng, T.Y. Hao, Y.F. Zhang, M.L. Xu, Polysulfone membranes clicked with poly (ethylene glycol) of high density and uniformity for oil/water emulsion purification: effects of tethered hydrogel microstructure, J. Membr. Sci., 470 (2014) 112–124.
[37] J. Li, D.M. Li, W.J. Li, H.Y. Li, H.D. She, F. Zha, Facile fabrication of underwater superoleophobic SiO_2 coated meshes for separation of polluted oils from corrosive and hot water, Sep. Purif. Technol., 168 (2016) 209–214.
[38] J. Li, L. Yan, W.F. Hu, D.M. Li, F. Zha, Z.Q. Lei, Facile fabrication of underwater superoleophobic TiO_2 coated mesh for highly efficient oil/water separation, Colloids Surf., A, 489 (2016) 441–446.